Cold Forging Behavior of Semicrystalline Polymers

Pratapkumar Nagarajan, Donggang Yao

Department of Mechanical Engineering, Oakland University, Rochester, Michigan

Received 16 January 2004; accepted 17 August 2004
DOI 10.1002/app.21516
Published online in Wiley InterScience (www.interscience.wiley.com).

ABSTRACT: Compared with molding processes, polymer solid-phase forming has several advantages. Particularly, polymer forging is able to reduce cycle time for thick parts, process difficult-to-mold materials, and enhance mechanical performance through self-reinforcment. Although much research has been carried out in the past on solid-phase forming, little has been done on polymer forging. This can be partially attributed to the lack of fundamental understanding of the process, e.g., lack of understanding on instantaneous recovery and viscoelastic recovery and lack of a modeling and simulation capability. In the present study, upsetting experiments were conducted to study the forging behavior of nylon. The instantaneous elastic recovery and the time-dependent postrecovery were found to be significantly affected by upsetting speed and dwell time. The dimensional recovery behavior of upset samples was interpreted using the Burgers model. The stress–strain data from the upsetting experiment was used in a viscoplastic simulation of forging a cylindrical hole. The simulation result about load versus forging displacement agrees well with that from the forging experiment. © 2005 Wiley Periodicals, Inc. J Appl Polym Sci 96: 764–771, 2005

Key words: viscoelastic properties; nylon; compression; solid-phase forming; recovery

INTRODUCTION

Thermoplastic polymers are typically processed using various thermoplastic molding processes, eg., injection molding, extrusion blow molding, compression molding, etc., in which the material is melted and shaped under pressure work.[1] These methods involve polymer fluidization by heating and shaping of the polymer inside the mold cavity, followed by cooling. In such processes the production rate is greatly affected by the cooling time because polymers in general have a poor thermal conductivity.[2] Other limitations of these processes arise from the difficulty in producing thick parts (the thickness usually limited to 3 mm)[2] and the difficulty in processing ultrahigh molecular weight polymers.[1]

Polymers have low stiffness and strength in comparison with other materials and consequently have to be improved in properties prior to their application. One effective way to enhance the mechanical properties of polymers is to introduce molecular orientations to the polymer matrix. In particular, stiffness and impact strength can be significantly improved by the employment of molecular orientations.[3] Orientations can be induced in polymers either in the melt, rubbery, or solid states.[1,3] For example, when the polymer is deformed below its softening temperature, the deformation-induced orientation will be locked in the final part.

In the past half century a considerable amount of work[1,3,4] has been done to develop processes different from the conventional molding process. These processes resemble more the solid-phase metalworking process, in which the work material does not have the fluidity to give rise to the type of fluid flow observed in processes such as extrusion and injection molding.[4] One advantage of polymer solid-phase forming is that the cooling time is considerably reduced. Further, solid-phase forming results in enhanced mechanical properties due to the self-reinforcing effect arising from molecular orientations. Polymer solid-phase forming has been successfully used in processing fibers, films, sheets, and shell structures.[3] Examples of solid-phase formed polymer articles are cold drawn high-strength high-modulus polymer fibers, stretch blow molded bottles, biaxially oriented films, etc. In general, these techniques involve elongational deformation of a relatively thin cross section. Very recently, the technology was adapted to cold extrusion of polymer rods under extremely high pressure.[5] The so-extruded rod has superb mechanical properties due to a high degree of self reinforcing.

Another polymer solid-phase forming technique is forging,[1,4] which utilizes compression force to shape a relatively thick material. Besides the general advantages associated with solid-phase forming polymer forging is able to produce discrete parts, to process difficult-to-mold polymers, and to manufacture thick wall sections. For example, difficult-to-mold polymers

Correspondence to: D. Yao (yao@oakland.edu).

such as ultrahigh molecular weight polyethylene can be processed using this technique. Despite these advantages, polymer forging has attracted much less attention than stretching or drawing based solid-phase formation processes. From the limited literature[1,4] about polymer forging, it is conjectured that the hindered development of the polymer forging process could be partially attributed to the lack of understanding of the deformation and recovery behavior of solid polymers during forging. Some qualitative findings related to the polymer forging behavior can be drawn from the literature.[1,4] It appears that springback remains the major problem. The severity of the springback problem is much greater than that for sheet forming processes because of the usual lack of symmetry and variation in section thickness in forging. The dimensional change of forged polymer occurs upon removal of the forging from the dies and during its storage at the room temperature. Such dimensional change varies with the change of materials, geometries, and process conditions. With the lack of understanding on the dimensional recovery process, it is hard to control the dimensional accuracy of forged polymer products. Further, such lack of understanding results in the lack of a suitable simulation capability for polymer forging.

From the fundamental point of view, the bulk deformation behavior of solid polymer during forging may be characterized using a direct compression test or an upsetting test. The related recent literature about deformation behavior of solid polymer under compression test is thus briefly reviewed in the following. Wang et al.[6] studied the deformation behavior of polypropylene (PP) under uniaxial compression. In their experiment, PP was subjected to compression at temperatures between T_g (glass transition temperature) and T_m (melting temperature) and the deformation responses were studied by performing an axisymmetric compression test. The friction was reduced by using a hot die and a proper lubricant. They found that the thermomechanical deformation of PP under compression was sensitive to temperature and strain rate. The stress–strain response was captured by an elastic yield at the early stage, a constant flow stress at the intermediate stage, and an orientation hardening at the final stage. Ray et al.[7] studied the stress–strain behavior of polyethylene (PE) and poly(ethylene-*co*-vinyl acetate (EVA) blends under compression with various strain rates and temperatures. They found that stress–strain plots consist of three parts, namely, elastic or Hookean region, region of chain slippage, and region of strain hardening, and these regions are significantly affected by the change of strain rate and temperature. Pluta et al.[8] subjected polypropylene to plain strain compression and the deformed structure was investigated using light microscopy and differential scanning calorimetry. It was found that the initial sperulitic morphology was destroyed and was transformed into stacks of crystalline lamellae rotating toward loading direction. The deformed sample showed an increase in the melting point compared with the undeformed sample. The effect of friction on the deformation behavior of polymer during compression has also been studied in the literature.[6,9,10] To reduce the amount of barreling a low coefficient of friction is often preferred. Lubricants can be used to reduce friction between the specimen and the platen.[6] Bruce et al.[9,10] studied the molecular orientation of both lubricated and unlubricated uniaxially compressed PP discs. In the unlubricated sample the orientation was found to be inhomogeneous and was dependent on the radial distance from the disk axis. In the lubricated sample the orientation texture was perpendicular to the compression direction.

It can be seen that most of the previous work regarding the behavior of solid polymer during compression is about the flow stress data, i.e., stress as a function of strain. However, the flow stress data are not able to offer any insight into the dimensional recovery process after forging of the material. Therefore, systematic studies on the postcompression behavior including elastic and viscoelastic recovery are needed to further the development of the polymer forging process. In the present study, upsetting experiments were conducted to study the deformation behavior of nylon during compression and the dimensional recovery behavior after compression. The effects of different process variables including strain rate and dwell time on the room temperature forging behavior of nylon were studied. The material data obtained from the upsetting experiment were used to predict the forging behavior of a cylindrical hole and to compare with experimental results.

EXPERIMENTAL

Similar to traditional metal forging processes, a high amount of ductility of the material is greatly desired in polymer forging. There is a wide variety of solid polymers available and the ductility of the material differs from one to another. Amorphous polymers with glass transition temperature (T_g) above room temperature generally are brittle. The ductility of these polymers increases as temperature increases and the polymer becomes a rubbery material above its T_g. The ductility of semicrystalline polymers is also significantly dependent on the temperature to which the polymer is subjected. The role of the T_g on the ductility depends on the amount of crystallinity of the polymer. Generally speaking, a semicrystalline with a T_g well below room temperature is a highly ductile polymer. Polyethylene, for example, is able to be elongated to more than 200% of its original length. In addition, the ductility of polymers also depends on the load configura-

tion. An amorphous polymer such as polystyrene, which is brittle under tensile testing, could exhibit a ductile fracture under compression testing.

A large amount of plasticity of the material is also highly desired in polymer forging. Although superplasticity can be achieved at elevated temperatures well above T_g for amorphous polymers and above melting temperature (T_m) for semicrystalline polymers, a polymer solid is characterized by poor plasticity or high elasticity at low temperatures. Polymer solids thus exhibit a high amount of elastic recovery after forging, which is the major problem in polymer forging.[4] Therefore, selection of a material with a low elastic recovery is a priority. In general, amorphous polymers show a high amount of elastic recovery compared to crystalline polymers and large deformation is possible only at temperatures close to T_g.[4] Hence, semicrystalline polymers are considered to be more suitable in polymer forging.

Three semicrystalline polymers, high density polyethylene (HDPE), polypropylene, and nylon 6.6, were compared in terms of the deformability and the amount of elastic recovery using an upsetting test, ie., direct compression test. All three polymers were obtained from McMaster Carr Supply Company and then were machined to a billet size of 19.05-mm diameter and 12.7-mm height. The upsetting tests were carried out at room temperature using a Carver press. The samples were instantaneously unloaded at different magnitudes of strain. To precisely set the stop position of the top platen, shim stocks were inserted between the two platens. By the variation of the thickness of the shim stock, the desired forging strain can be prescribed. Although nylon required the highest load among the three polymers, the deformation of nylon was found to be the most uniform with the least amount of barreling effect. Furthermore, nylon exhibited the lowest amount of elastic recovery at various magnitudes of strains as shown in Figure 1. The elastic recovery, ξ, is defined by the following equation:

$$\xi = \frac{\varepsilon_{forging} - \varepsilon_{residual}}{\varepsilon_{forging}} \times 100 \qquad (1)$$

where $\varepsilon_{forging}$ is the total true strain the polymer is subjected to during forging and $\varepsilon_{residual}$ is the residual strain after instantaneous elastic recovery.

To investigate the temperature effect on the elastic recovery, upsetting experiments of nylon 6.6 at different operating temperatures were conducted. The sample was heated to a predetermined temperature and forged between two platens of the Carver press, which were maintained at the same temperature as that of the polymer billet. The temperature of the billets was varied from room temperature to 100°C. The temperature was found to have a profound effect on the instantaneous elastic recovery of the forged samples, as shown in Figure 2. The glass transition temperature of nylon 6.6 is around 50°C. It can be seen from the figure that the amount of elastic recovery increases as the temperature approaches and exceeds T_g and then decreases again when the temperature further increases. With the temperature range tested, the room temperature gives rise to the lowest amount of elastic recovery. The higher amount of elastic recovery above T_g may be attributed to the rubbery behavior of the amorphous portion in the polymer. The data in Figure 1 can also be explained using the temperature effect. Among the three polymers, HDPE has the lowest T_g and is a relatively rubbery material at room temperature. Therefore, HDPE exhibits the highest amount of elastic recovery among the three.

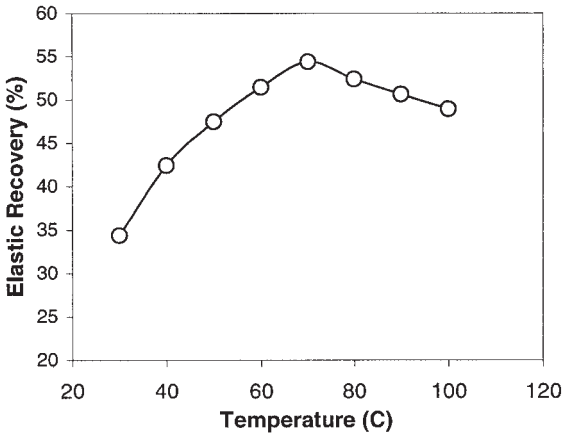

Figure 2 Instantaneous recovery of nylon at various temperatures.

Based on the above preliminary experiments for material selection and operation temperature determination, nylon 6.6 was chosen as the material for further study of its forging-related behavior. Room temperature was used throughout the remaining experiments. Stress–strain relations, elastic recovery, postrecovery, and stress relaxation were studied and the effects of upsetting speed and dwell time on dimensional recovery were investigated. An Instron universal testing machine was used for these experiments. Each experiment was repeated at least three times.

RESULTS AND DISCUSSION

Figure 3 shows the stress–strain relation for nylon unloaded at different magnitudes of strain and at a constant upsetting speed of 14.2 mm/min. The stress–strain curve is characterized by an initial elastic yield, followed by stain hardening and strain softening. The elastically recovered strain for a specific forging strain can be directly read from the plot. For example, the

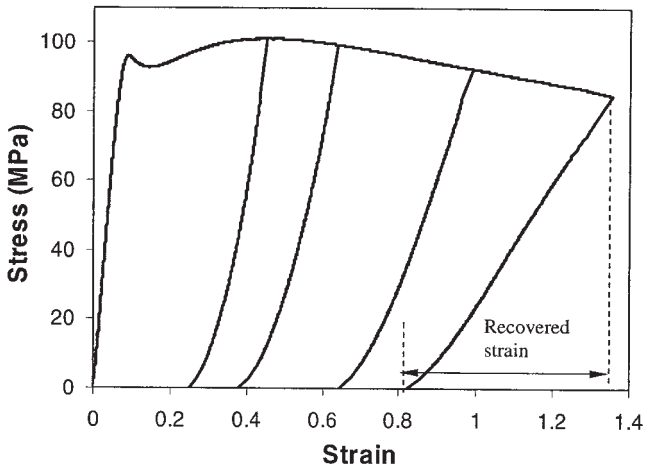

Figure 3 Stress–strain relations of nylon at an upsetting speed of 14.2 mm/min.

elastically recovered strain for a compression strain of 1.35 (corresponding to a reduction of 75% of the sample height) is around 0.55. Therefore, about 40% of the total forging strain was elastically recovered after unloading. The elastic recovery modulus, i.e., the slope of the recovery curve, was found to be strain dependent. A strain-softening effect was observed for the elastic recovery process. The elastic recovery modulus decreases as the strain increases. In comparison, for an ideal material with an elastic recovery modulus that is independent on the applied strain, the elastically recovered strain will be proportional to the applied stress.

The effect of the upsetting speed on the stress–strain curve was also studied. Figure 4 shows stress–strain curves for three different speeds, i.e., 3.6, 14.2, and 56.9 mm/min. The stress–strain curves were recorded upon unloading the sample at a strain of 1.15. The upsetting speed was found to have some effect on the stress–strain relations. Strain rate hardening effect was observed on the yielding stress. Dependence of the elastic recovery modulus on the upsetting speed was also observed.

The instantaneous and time-dependent dimensional changes of the forgings were measured and recorded immediately upon unloading at a sample height of 5.66 mm and periodically with time for a period of 60 h. After unloading, the forging instantaneously recovered to 8.11, 7.95, and 8.12 mm, respectively, for upsetting speeds of 3.6, 14.2, and 56.9 mm/min. Both instantaneous and time-dependent dimensional changes of the forgings were found to be a function of upsetting speed and thus dependent on the strain rate. Among the three upsetting speeds, the middle speed gave rise to the lowest instantaneous elastic recovery. The time-dependent dimensional changes were found to be higher for lower upsetting speeds, as shown in Figure 5. It can also be seen that the majority of the time-dependent recovery occurred during the first 90 min.

The effect of the dwell time on the instantaneous elastic recovery is shown in Figure 6. The samples were forged to 6.35 mm at a speed of 14.2 mm/min and kept at that dimension under the pressure for a dwell time. The elastic recovery is defined by eq. (1). The dwell time varied from 0 to 20 mins. With the employment of the dwell time, the amount of instantaneous elastic recovery of the forging was reduced from 37 to 26%, as shown in Fig. 6.

Figure 7 shows the stress relaxation process for nylon samples compressed to a height of 8.5 mm and held at this height by the Instron machine. The starting stress for all three speeds is around 90 MPa. The upsetting speed was found to affect the stress relaxation process of the forged specimen. The sample forged at the middle upsetting speed relaxed to a

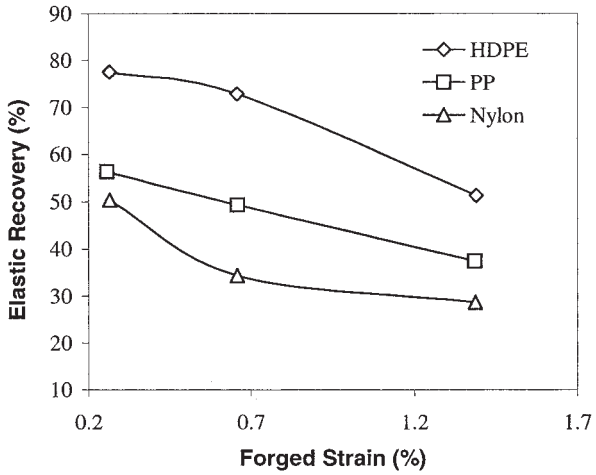

Figure 1 Elastic recovery upon unloading at different reductions for HDPE, nylon, and PP.

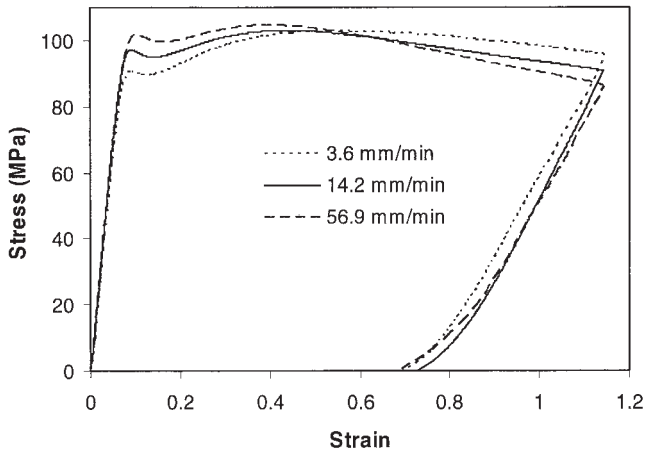

Figure 4 Stress–strain curves of nylon for different compression speeds.

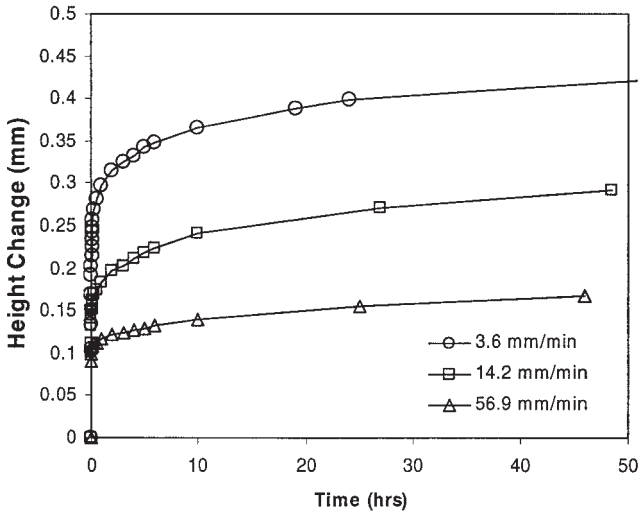

Figure 5 Time-dependent dimensional changes after compression.

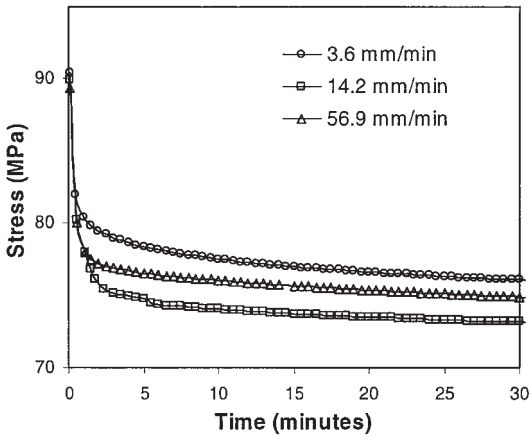

Figure 7 Stress relaxations after samples were compressed to a height of 8.5 mm at various speeds.

lower stress level than the sample forged at the other two speeds.

To explain the above dimensional recovery behavior, two of the simplest models for viscoelastic materials, i.e., the Maxwell model and the Kelvin model, were studied first. The Maxwell model, i.e., a spring in series with a dashpot, is able to predict the elastic recovery phenomenon when a sample is compressed at a constant strain rate and then immediately unloaded. For a compression strain rate of $\dot{\varepsilon}$ and a total compression strain of ε_0, the Maxwell model predicts the following compression stress upon unloading:

$$\sigma = \eta\dot{\varepsilon}(1 - e^{-\varepsilon_0/\dot{\varepsilon}\lambda}) \tag{2}$$

where E is the modulus of the spring and $\lambda = \eta/E$ is the relaxation time. When the sample is unloaded instantaneously, the above stress inside the spring will be instantaneously released to zero, giving rise to the instantaneous elastic recovery. The amount of strain recovered instantaneously at the unloading instant, ε_e, can thus be represented as:

$$\varepsilon_e = \lambda\dot{\varepsilon}(1 - e^{-\varepsilon_0/\dot{\varepsilon}\lambda}) \tag{3}$$

From the above equation, the instantaneously recovered strain increases with the increase of strain rate. The Maxwell model is also capable of predicting the effect of dwell time on the instantaneous elastic recovery. As the dwell time increases, the stress inside the spring–dashpot set decreases, which in turn reduces the elastic recovery. The data in Figure 6 about the effect of the dwell time agree with this prediction. The Maxwell model, however, cannot predict the time-dependent postrecovery.

Different from the Maxwell model, the Kelvin model, i.e., a spring in parallel with a dashpot, cannot predict the elastic recovery process, but is able to predict the time-dependent postrecovery process. For the same compression loading configuration, the Kelvin model predicts the following recovered strain, ε_p:

$$\varepsilon_p(t) = \varepsilon_0(1 - e^{-t/\tau}), \tag{4}$$

where t is the time zeroed at the unloading instant and $\tau = \eta/E$ is called the retardation time for the Kelvin model. At $t = 0$, the recovered strain is zero. It is further noted that the time-dependent postrecovery process is independent on the strain rate during compression, which deviates from the findings in the present experiments (Fig. 5).

Either the Maxwell model or the Kelvin model is able to qualitatively explain part of the recovery process, but neither is able to explain both the elastic recovery phenomenon and the time-dependent recov-

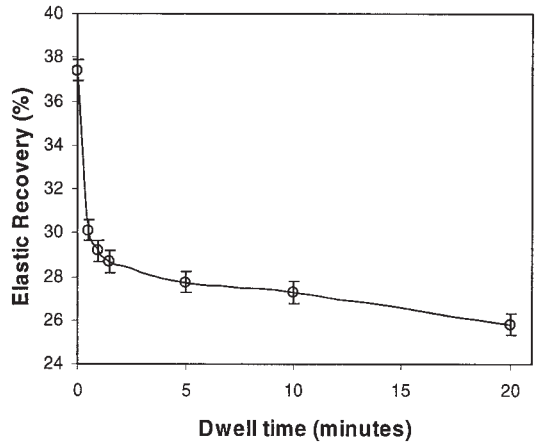

Figure 6 Effect of dwell time on the instantaneous elastic recovery.

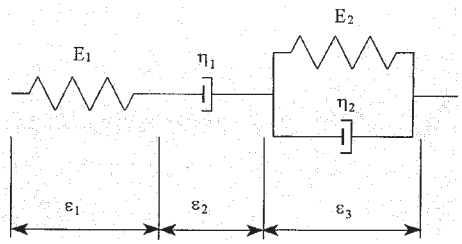

Figure 8 The Burgers model.

ery phenomenon. It is thus conjectured that a model combining the Maxwell model and the Kelvin model may be capable of predicting the entire recovery process observed in the upsetting experiment. The resulting model is the Burgers model,[11] as shown in Figure 8. The Burgers model in the literature was used to predict the viscoelastic response of an amorphous polymer, particularly stress relaxation and creeping behaviors. The governing equation for this model is

$$\sigma + \left(\frac{\eta_1}{G_2} + \frac{\eta_2}{G_2} + \frac{\eta_1}{G_1}\right)\dot{\sigma} + \frac{\eta_1\eta_2}{G_1G_2}\ddot{\sigma} = \frac{\eta_1\eta_2}{G_2}\ddot{\varepsilon} + \eta_1\dot{\varepsilon} \quad (5)$$

By solving the above equation with boundary conditions, the stress at the unloading instant for a specimen compressed under a constant strain rate of $\dot{\varepsilon}$ and with a total strain of ε_0 can be written as:

$$\sigma(0) = \eta_1\dot{\varepsilon} + \frac{E_1\dot{\varepsilon} - \eta_2\beta}{\beta - \alpha}e^{-\frac{\alpha\varepsilon_0}{\dot{\varepsilon}}} + \frac{-E_1\dot{\varepsilon} + \eta_2\alpha}{\beta - \alpha}e^{-\frac{\beta\varepsilon_0}{\dot{\varepsilon}}} \quad (6)$$

with

$$\begin{Bmatrix} \alpha \\ \beta \end{Bmatrix} = \frac{\eta_1^2}{E_1\eta_2} + \frac{E_2}{\eta_1} + \frac{E_1}{\eta_1} \pm \sqrt{\left(\frac{\eta_1^2}{E_1\eta_2} + \frac{E_2}{\eta_1} + \frac{E_1}{\eta_1}\right)^2 - \frac{4E_1E_2}{\eta_1\eta_2}}. \quad (7)$$

At the unloading instant, the stress inside the first spring will instantaneously release, resulting in the elastically recovered strain. Therefore, the elastically recovered strain is calculated as

$$\varepsilon_e = \frac{\sigma(0)}{E_1} \quad (8)$$

The total strain upon unloading inside the Kelvin part, i.e., ε_3 referring to Figure 8, can also be computed as

$$\varepsilon_3(0) = \frac{\sigma(0)\left(1 + \frac{\eta_2}{\eta_1}\right) - \left(\eta_2\dot{\varepsilon} + \left|\frac{\eta_2\dot{\sigma}(0)}{E_1}\right|\right)}{E_2}. \quad (9)$$

The poststrain recovery process can thus be modeled as.

$$\varepsilon_p(t) = \varepsilon_3(t) = \varepsilon_3(0)(1 - e^{-t/\tau}). \quad (10)$$

Based on the Burgers model, the integrated strain recovery process can be modeled and the experimental upsetting results can be qualitatively explained. From Eqs. (6) and (8), it is known that the amount of instantaneous elastic recovery decreases with the decrease of strain rate. In the actual experiment, with the sample compressed to about half of its original height and unloaded, the elastic recovery decreased when the upsetting speed decreased from 56.9 to 14.2 mm/min. This result is confined with the Burgers model. However, when the speed further decreased to 3.6 mm/min, the measured instantaneous recovery increased, which violates the Burgers model. Careful examination of the experiment procedure revealed the reason for this discrepancy. Because the Instron machine uses a fixed speed for both loading and unloading, the unloading process will take more time when a lower speed is used. The actual unloading time for the speed of 3.6 mm/min was about 40 s. During this period, postrecovery occurred, which adds to the measured elastic recovery.

The Burgers model can be used to predict the influence of upsetting speed on the postrecovery process. From eq. (9), there are two competing terms on the numerator; the first term increases with the increase of strain rate while the second term decreases with the increase of strain rate. Whether ε_3 (0), and consequently the time-dependent recovery, increases with the increase of strain rate depends on the collection of the parameters for the Burgers model. From the experimental data shown in Figure 5, the amount of time-dependent recovery decreased with the increase of upsetting speed. To predict the same trend as the experimental data, proper parameters of the Burgers model is needed. One specific case that can be used is $\eta_2 \gg \eta_1$ and $E_2 \ll E_1$.

POLYMER FORGING SIMULATION

The Burgers model is able to qualitatively explain the elastic recovery process and the postrecovery process. However, an accurate quantitative model is still lacking and needs to be developed in the future. Without such accurate modeling, simulation of the dimensional recovery of forged polymer products is difficult. On the other hand, simulation for metal forging processes has been well developed during the past several

decades. The standard routine for simulating metal forging employs the viscoplastic formulation.[12–14] It is clear that the viscoplastic formulation by itself is not capable of predicting the time-dependent dimensional recovery. However, it may be prudent to examine the suitability of such a formulation for the prediction of the deformation behavior of the polymer during the forging stage. With future advancement on the understanding of the strain and strain rate dependent recovery modulus and the postrecovery process, the viscoplastic formulation may be modified to incorporate the new findings. The viscoplastic formulation[12–14] is given in detail as follows.

Governing equations (in indicial notation)

Mass conservation equation

$$v_{i'i} = 0 \tag{11}$$

where v_i is a velocity component and "'" denotes the differentiation.

Force balance equilibrium equation

$$\sigma_{ij'j}=0 \tag{12}$$

where σ_{ij} is a stress component.

Strain rate–velocity relation:

$$\sigma'_{ij} = \frac{1}{2}\,(v_{i,j} + v_{j,i}), \tag{13}$$

where $\dot{\varepsilon}_{ij}$ is a strain rate component.

Constitutive relation:

$$\sigma'_{ij} = \frac{2\tilde{\sigma}}{3\dot{\tilde{\varepsilon}}}\,\dot{\varepsilon}_{ij} \tag{14}$$

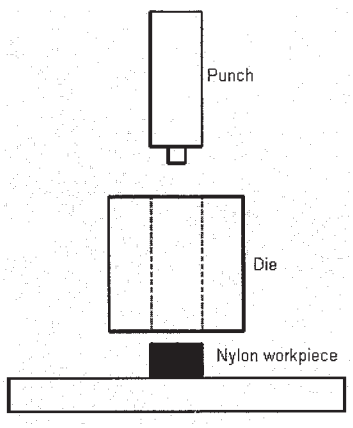

Figure 9 Setup for forging a cylindrical hole.

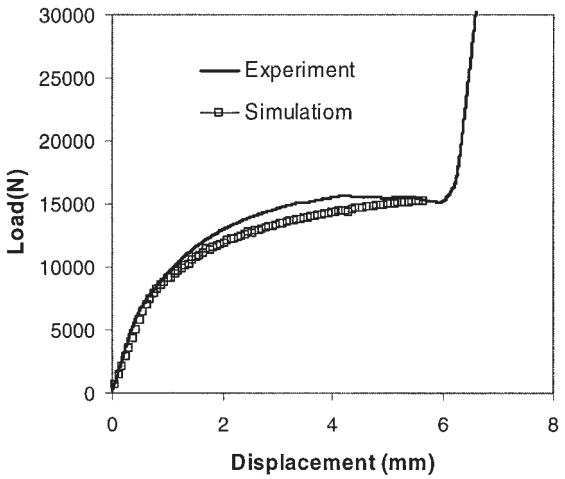

Figure 10 Comparison of load-displacement data.

where $\sigma'_{ij} = \sigma_{ij} - 1/3\delta_{ij}\sigma_{ij}$ is the deviatoric stress, and $\tilde{\sigma}$ and $\tilde{\varepsilon}$ are defined by $\sqrt{3/2\sigma'_{ij}\sigma'_{ij}}$ and $\sqrt{3/2\varepsilon_{ij}\dot{\varepsilon}_{ij}}$, respectively. The flow stress $\tilde{\sigma}$ for polymers is a function of strain, strain rate, and temperature.

The test geometry for the polymer forging simulation is a cylindrical hole with a diameter of 6.35 mm and a depth of 6.35 mm on an initial billet size of 19.05-mm diameter and 12.7-mm height. A commercially available finite element code, MSC Marc®, was used to implement the large deformation viscoplastic approach. The forging speed used in the simulation is 14.2 mm/min. The true stress–strain data at this speed as shown in Figure 4 were used to model the flow stress. An actual experiment was carried out to compare with the simulation result. The die-punch set used for this forging experiment is shown in Figure 9. The nylon billet was constrained inside the fixture with the same constraints and the hole was forged at the same speed as used in the simulation. The load displacement data were recorded during the experiment. From the results in Figure 10, the load displacement data obtained from the simulation agree very well with the actual experimental result. The sudden increase of load in the experiment is due to the full contact of the punch shoulder with the billet.

CONCLUSION

The deformation and dimensional recovery characteristics of nylon during forging and postforging were investigated in a series of upsetting experiments. The dimensional changes after upsetting were found to be a function of upsetting speed, dwell time, magnitude of strain applied, and the operation temperature. The overall recovery can be reduced by the application of a higher upsetting speed and an appropriate dwell time during forging. The general behavior of nylon during forging and postforging can be qualitatively

predicted using the Burgers model. The load-displacement data for forging a cylindrical hole predicted using the viscoplastic formulation agree well with the experimental result. With a considerable amount of research in the future toward fundamental understanding of the dimensional recovery process of forged solid polymers, an integrated routine for simulating the complete polymer forging process can be developed.

References

1. Titus, J. B. In Plastics Report; Plastics Technical Evaluation Center: Picatinny Arsenal, NJ, 1972.
2. Lo, Y.-C. Solid Phase Flow Behavior of Thermoplastics; University of Wisconsin: Madison, 1984.
3. Ward, I. M.; Coates, P. D.; Dumoulin, M. M. Solid Phase Processing of Polymers; Hanser Gardner Publications: Munich, 2000.
4. Kulkarni, M. Polym Eng Sci 1979, 19, 474.
5. Huang, H.-X. Polym Eng Sci 1998, 38, 1805.
6. Wang, P. T.; Chen-Tsai, C. H.; Sample, V. M. J Elastomers Plastics 1990, 22, 32.
7. Ray, I.; Khastgir, D.; Mukunda, P. G. Angew. Makromol Chem 1993, 205, 59.
8. Pluta, M.; Bartczak, Z.; Galeski, A. Polymer, 2000, 41, 2271.
9. Bruce, G. D.; Weatherly, G. C.; Vancso, G. J. Angew. Makromol Chem 1993, 205, 161.
10. Bruce, G. D.; Weatherly, G. C.; Vancso, G. J. Angew. Makromole Chem 1993, 205, 177
11. Progelhof, R. C.; Throne, J. L. Polymer Engineering Principles; Hanser Publishers: Munich, 1993.
12. Lee, C. H.; Kobayashi, S. ASME Trans J Eng Int 1973, 95, 865.
13. Rebeldo, N.; Kobayashi, S. Int J Mech Sci 1980, 22, 699.
14. Oh, S. I. Int J Mech Sci 1982, 24, 479.